Mekanika: Majalah Ilmiah Mekanika

.

Optimization of Photovoltaic Performance Through the Integration of a Heatsink–Blower Cooling System Under Solar Simulator Testing Conditions

Godlisten Gladstone Kombe[1], Buruhan Haji Shame[2], Muh. Farhan Atha Farid[3], Tyo Febrino Fernandio Prasetyo[3], Nabella Sofa Nur Afiqoh[3], Nindia Nova Novena[3], Yuki Trsinoaji[3], Mangisi Larixon Lumban Gaol[3], Febrianto Sinaga[3], Singgih Dwi Prasetyo[3*]

1 Department of Petroleum and Energy Engineering, The University of Dodoma, Dodoma, Tanzania

2 The Ministry of Infrastructure, Communication and Transportation, Zanzibar, Tanzania

3 Power Plant Engineering Technology, State University of Malang, Malang, Indonesia

*Corresponding Author's email address: singgih.prasetyo.fv@um.ac.id

Keywords:
Photovoltaic
Cooling system
Heatsink

Abstract
This study examines the impact of a heatsink-based cooling system, combined with forced airflow, on the thermal and electrical performance of a photovoltaic (PV) module under controlled irradiance conditions provided by a solar simulator. The cooling configuration employed is energy-efficient and straightforward, utilizing active convection enhanced by a blower in selected trials. Two primary conditions were compared: PV without cooling and PV with different cooling configurations. The experimental results indicate that the PV + Heatsink + Blower configuration achieved the highest average electrical efficiency of 13.43%, whereas the PV Only configuration recorded the lowest, 12.45%. This difference demonstrates that temperature regulation through a combination of heatsink and assisted airflow significantly improves electrical energy conversion. Furthermore, maintaining a lower, more stable operating temperature contributes to consistent power output and reduces heat accumulation, which can accelerate performance degradation. Overall, the findings suggest that integrating a low-energy, straightforward cooling design can be an effective strategy to enhance PV performance, particularly in testing environments that use a solar simulator.

1 Introduction

The development of photovoltaic (PV) technology requires testing methods that can consistently and measurably represent operational conditions [1-3]. In this context, solar simulators have become essential because they enable controlled performance evaluation without dependence on fluctuating natural solar irradiance [4,5]. By providing adjustable radiation intensity and spectral characteristics, solar simulators

https://dx.doi.org/10.20961/mekanika.v25i1.114555

Revised 17 March 2026; received in revised version 20 March 2026; Accepted 21 March 2026
Available Online 30 April 2026

2579-3144

ensure repeatable testing conditions. However, high-intensity artificial radiation often increases PV module temperatures, reducing energy conversion efficiency [6, 7].

Thermal stabilization is therefore a critical component in the design of solar simulator–based testing systems [6]. One widely adopted solution is the use of a heatsink as an active cooling mechanism, which enhances heat dissipation through conduction and convection [8, 9]. Uncontrolled temperature rise can significantly affect key electrical parameters such as short-circuit current, open-circuit voltage, and maximum power point, thereby compromising measurement accuracy [10, 11]. Consequently, integrating an appropriately designed heatsink is essential to ensure reliable and valid PV performance characterization under controlled irradiation [12].

As summarized in Table 1, previous studies have explored various cooling strategies, including aluminum-based nanofluids, advanced heatsink geometries, phase-change materials, and thermoelectric cooling systems [13, 14]. While these methods effectively improve thermal regulation and output stability, many involve complex configurations or additional energy consumption. This highlights the need for simpler, more energy-efficient cooling solutions that can be readily implemented in photovoltaic testing systems. Accordingly, the present study addresses this gap by developing a practical active-cooling approach to accurately and repeatably evaluate PV performance under simulated solar conditions.

Table 1. Summary of state-of-the-art cooling technologies for photovoltaic performance enhancement

Reference	Method	Key Finding
[14]	Experimental study of PV cooling using **a heatsink combined with 2% aluminum nanofluid,** including temperature, power, and efficiency measurements.	Surface temperature reduction of up to **13–16 °C** and panel efficiency/output power improvement of approximately **13.5%** and **13.7%**, respectively. The study demonstrates that Al-based nanofluid is highly effective in enhancing PV performance.
[15]	Experimental study using **mini-channel heatsinks**, **jet impingement, hybrid heatsinks**, and **variations** in flow rate.	The best cooling performance was achieved with a hybrid heatsink, which significantly improved panel efficiency while maintaining lower operating temperatures. The results highlight the critical role of structured thermal design.
[16]	Experimental investigation of PV cooling using **PCM (paraffin wax)** with various fin configurations.	Circular **fins** provided the best cooling performance. PCM significantly reduced panel temperature and improved electrical efficiency.
[17]	Experimental study of solar panel cooling using a **thermoelectric cooler (TEC)** based on Peltier modules with thermal performance analysis.	The TEC system successfully reduced PV surface temperature and increased power output; however, additional thermal management is required to maintain long-term efficiency.
[18]	Experimental study of PV cooling under hot climate conditions (UAE) using **active cooling systems** with thermal performance analysis.	Active cooling effectively reduced panel temperature in extreme environments, improved output stability, and extended PV module lifespan.

2 Experimental Methods

This study employed an experimental approach to evaluate the thermal and electrical performance of a photovoltaic (PV) module equipped with an active heatsink under controlled irradiance from a solar simulator, as illustrated in Figure 1. The solar simulator was operated to provide stable illumination. Afterward, the PV module was positioned beneath the light source with the heatsink attached to its rear surface to enhance active heat dissipation. In selected trials, a blower fan was added to introduce forced convection for comparative analysis. Module temperature was measured using a non-contact infrared thermometer, while voltage and current outputs were recorded using a digital avometer. All measurements were conducted under identical irradiance conditions to ensure that performance variations were solely attributable to the applied cooling configurations. The resulting data were analyzed to assess the heatsink's effectiveness in stabilizing PV temperature and improving electrical efficiency under simulated solar radiation.

2.1 Heatsink-based active cooling configuration

This experiment aims to evaluate the effect of a heatsink-based active cooling system on the thermal and electrical performance of a photovoltaic (PV) module under controlled irradiance provided by a solar simulator. An aluminum heatsink was attached to the rear surface of the PV module using a high-thermal-conductivity adhesive to ensure effective heat transfer from the PV cells to the cooling fins. During irradiation, heat generated by the cells was conducted toward the heatsink and dissipated into the surrounding air through natural convection, thereby reducing the module's operating temperature. Surface temperature was measured with a non-contact infrared thermometer, while voltage and current were recorded with a digital avometer. This configuration represents a simple, energy-free cooling approach that effectively enhances temperature stability during PV performance testing under constant irradiance.

The cooling system consists of a steel grid-type heatsink combined with a blower to enhance forced convection. The heatsink is fabricated from 3 cm × 3 cm hollow steel sections with overall dimensions of approximately 610 mm × 580 mm. The lattice configuration increases the effective surface area for heat dissipation. The structure is mounted on the rear surface of the PV module to promote conductive heat transfer from the backsheet to the steel grid. A blower is installed to generate forced airflow across the heatsink surface, thereby improving convective heat transfer compared to natural convection.

2.2 Fundamental mathematical formulation

Performance analysis was conducted on a 50 Wp photovoltaic panel tested under a 500 W halogen-based solar simulator. The evaluated parameters include voltage, current, electrical power, electrical efficiency, and thermal behavior, which collectively describe the panel's energy conversion performance. All parameters were calculated using standard equations commonly applied in photovoltaic characterization. The variation in output voltage due to changes in cell temperature is expressed as Equation (1) [19-21].

$$V = V_{ref}[1 + \alpha_V(T - Tref)] \quad (1)$$

where V_{ref} is the reference voltage, α_V is the voltage temperature coefficient, and T is the operating temperature of the PV module. The change in output current resulting from temperature variation is given by Equation (2) [22-24].

$$I = I_{ref}[1 + \alpha_I(T - Tref)] \quad (2)$$

where Irefrepresents the reference current at 25 °C and $\alpha_I$is the current temperature coefficient. The electrical power output of the PV module is calculated as shown in Equation (3) [25,26].

$$P = V \times I \tag{3}$$

During the experiment, the PV module was connected to a fixed lamp load. Voltage and current were measured across the load using a digital multimeter. The electrical operating point was therefore determined by the load characteristics rather than Maximum Power Point Tracking (MPPT). No I–V sweep was conducted; hence, the reported power values represent operating-point power under controlled load conditions rather than true maximum power (P_{max}). The same lamp load was maintained for all configurations to ensure a consistent comparison [27]. The input power is calculated as in Equation (4).

$$P_{in} = G \times A \tag{4}$$

where, G is the measured irradiance (W/m^2) at the PV surface and A is the active area of the PV module (m^2). Irradiance measurements were conducted at the module plane to ensure an accurate representation of incident power [28,29].The electrical efficiency of the photovoltaic module is therefore defined as Equation (5).

$$\eta_{elec} = \frac{Pout}{G \times A} \times 100\% \tag{5}$$

This approach ensures that efficiency values are physically consistent with the actual incident radiation rather than the nominal lamp rating.

In this study, no heat recovery mechanism is employed; therefore, thermal performance is evaluated based on temperature behavior rather than thermal efficiency. The cooling effectiveness is assessed through temperature reduction relative to the baseline configuration in Equation (6) [30,31]:

$$\Delta T = T_{baseline} - T_{cooling} \tag{6}$$

where, $T_{baseline}$ represents the steady-state temperature of the PV-only configuration and $T_{cooling}$ represents the temperature under heatsink or hybrid configurations. This parameter directly quantifies the thermal stabilization capability of the proposed cooling design without implying sound thermal energy output [32].

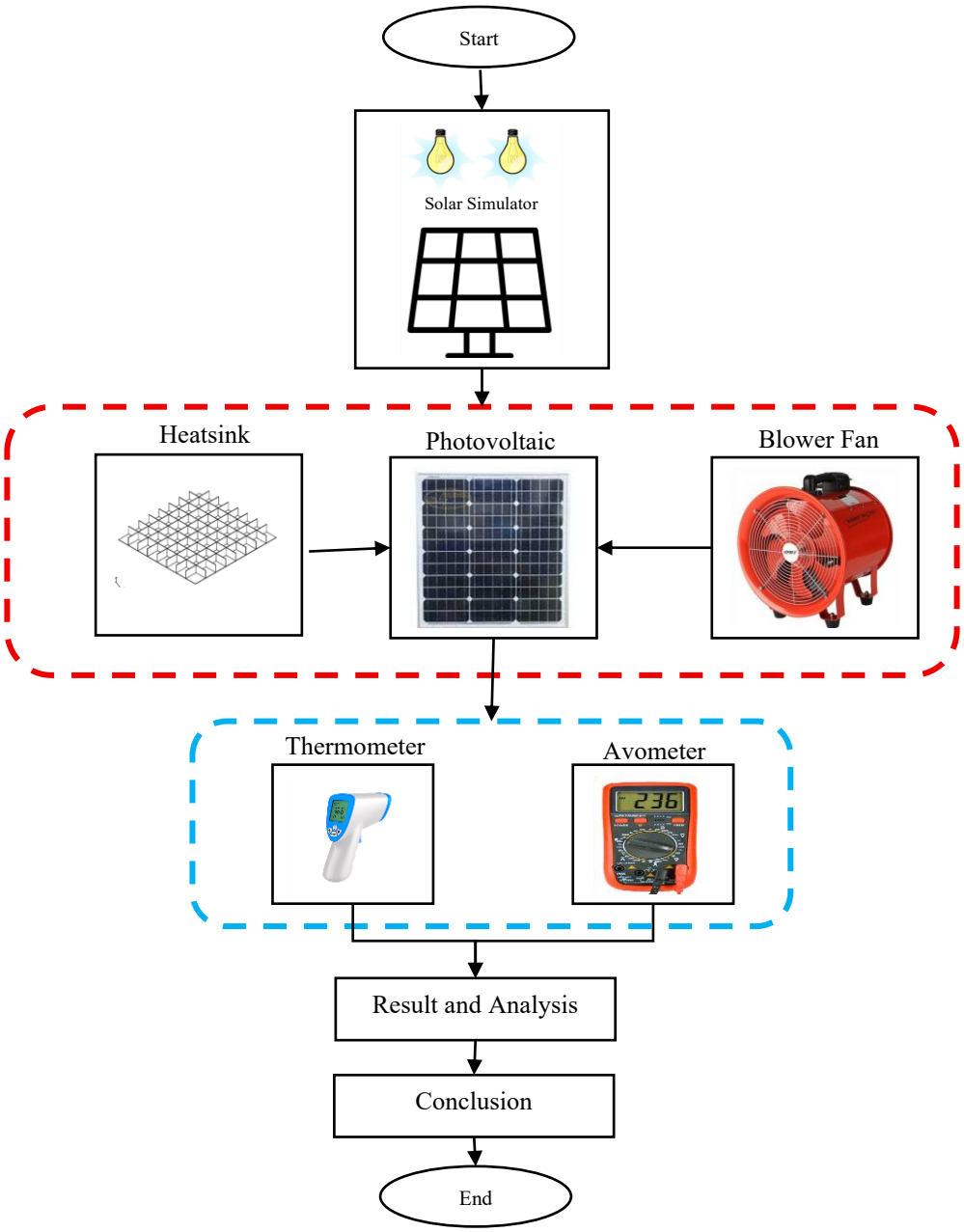

Figure 1. Experimental workflow of the solar simulator–based PV heatsink testing setup

3 Results and Discussion

The temperature response of the photovoltaic module under different cooling configurations shows a clear distinction, as illustrated in Figure 2. The PV-only configuration reached the highest operating temperature, rising from approximately 28 °C to nearly 75 °C after 180 minutes, whereas the active heatsink limited the temperature to about 52 °C, reducing it by more than 20 °C. The blower-only configuration exhibited intermediate performance, with temperatures stabilizing near 65 °C, whereas the hybrid PV + Heatsink + Blower system achieved the most significant reduction, maintaining temperatures within 30–40 °C. This corresponds to an overall decrease of approximately 35 °C compared to PV Only, confirming the effectiveness of combining conductive heat spreading with forced convection.

The electrical performance trends shown in Figure 3 (a)–(c) and Figure 4 (a)–(b) closely follow the thermal behavior of the module. The current exhibited minimal variation, with a maximum difference of only 0.057 A, reflecting its weak temperature dependence. In contrast, the voltage showed strong sensitivity to thermal regulation, decreasing from approximately 17.05 V in the hybrid configuration to 14.95 V in the PV-only configuration. As a result, the PV + Heatsink + Blower configuration achieved the highest power output of roughly 47.6 W and an electrical efficiency of 13.43%, compared to 43.0 W and 12.45% for the PV-only configuration. Conversely, thermal efficiency decreased as cooling improved, indicating that enhanced electrical performance is primarily driven by effective heat removal rather than by heat retention under controlled solar-simulator conditions.

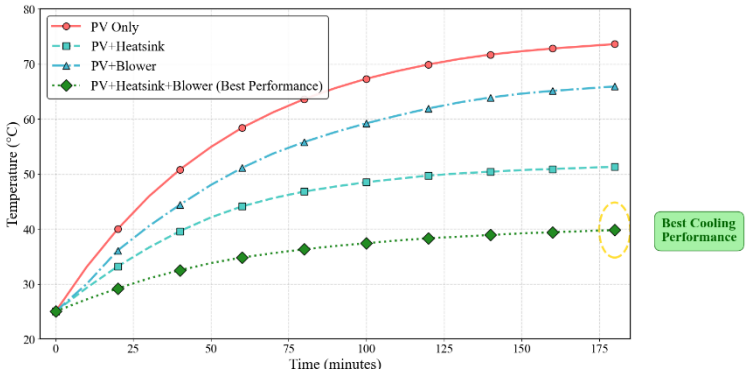

Figure 2. Thermal behavior transformation of pv modules across cooling strategies

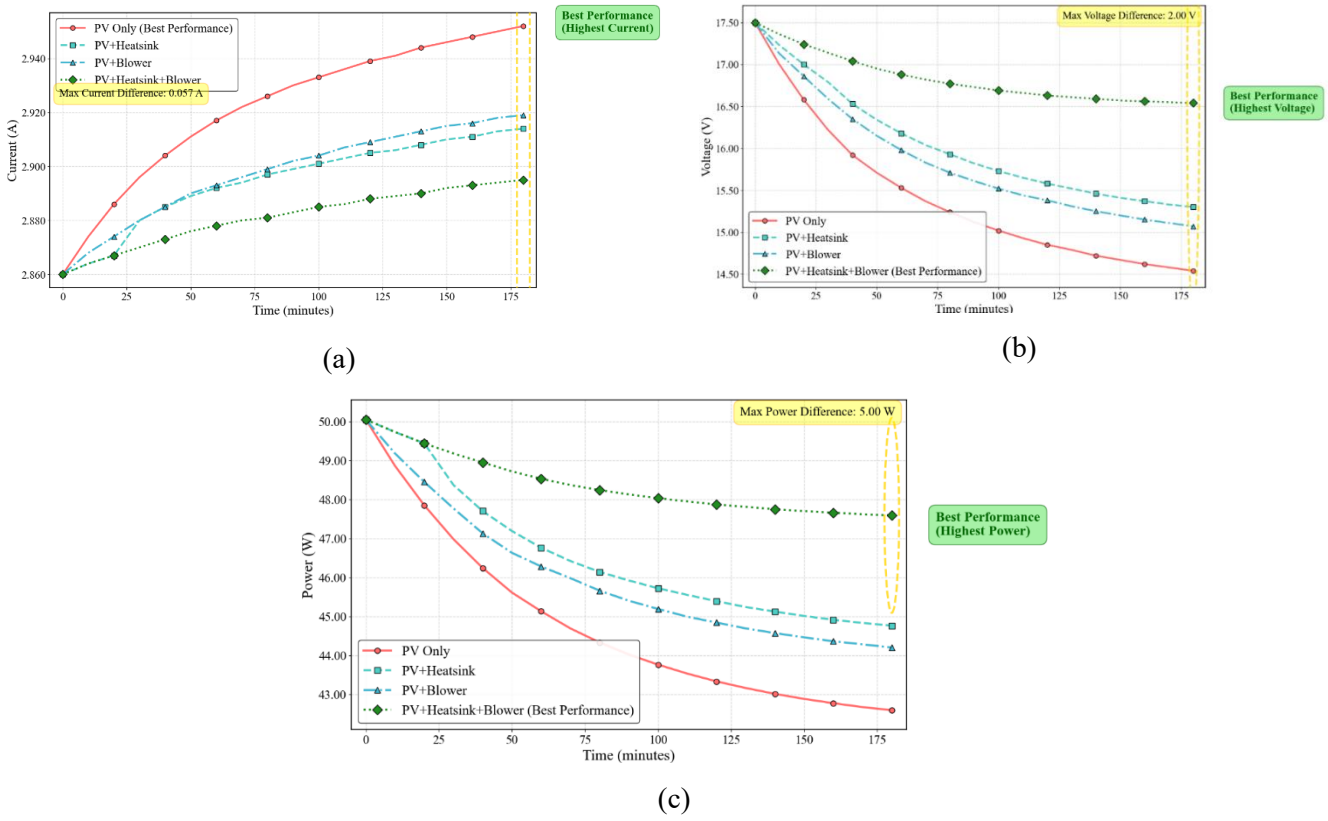

Figure 3. Performance characteristics: (a) current performance of PV with different cooling configurations, (b) voltage performance of PV with different cooling configurations, and (c) power output performance of PV with different cooling configurations

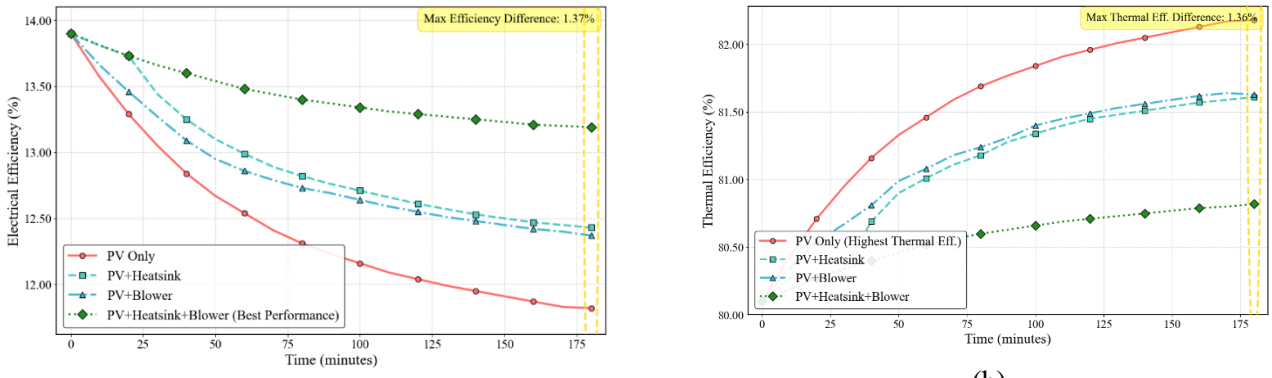

(a) (b)

Figure 4. Efficiency analysis: (a) electrical efficiency of PV with different cooling configurations and (b) thermal efficiency of PV with different cooling configurations.

The electrical efficiency summary in Table 2 demonstrates apparent performance differences among the four cooling configurations. The PV-only system exhibited the lowest average electrical efficiency at 12.45% with the highest variance (0.3863), indicating strong temperature-induced voltage degradation and unstable output. Moderate improvements were observed with the PV + Heatsink (12.93%) and PV + Blower (12.83%) configurations. In contrast, the PV + Heatsink + Blower system achieved the highest efficiency at 13.43% with the lowest variance (0.0475), reflecting both superior performance and stability. The Analysis of Variance (ANOVA) results in Table 3 confirm that cooling configuration has a statistically significant effect on electrical efficiency ($F = 108.48 > F\text{-crit} = 2.77$, $p = 7.58 \times 10^{-23}$). At the same time, experimental time also significantly influences efficiency due to progressive thermal accumulation

Table 2. Summary of experiment data by electrical efficiency

Summary	Count	Sum	Average	Variance
0	4	55.6	13.9	0
10	4	54.85	13.7125	0.014025
20	4	54.21	13.5525	0.046825
30	4	53.42	13.355	0.066833
40	4	52.78	13.195	0.101367
50	4	52.26	13.065	0.132033
60	4	51.87	12.9675	0.152492
70	4	51.53	12.8825	0.180892
80	4	51.26	12.815	0.2015
90	4	51.05	12.7625	0.219292
100	4	50.85	12.7125	0.234758
110	4	50.65	12.6625	0.250758
120	4	50.49	12.6225	0.263425
130	4	50.34	12.585	0.276367
140	4	50.21	12.5525	0.285092

Table 2. *Cont.*

Summary	Count	Sum	Average	Variance
	4	50.09	12.5225	0.293825
160	4	49.97	12.4925	0.302692
170	4	49.88	12.47	0.315933
180	4	49.81	12.4525	0.317092
PV Only	19	236.47	12.44579	0.386281
PV + Heatsink	19	245.62	12.92737	0.232387
PV + Blower	19	243.81	12.83211	0.202462
PV + Heatsink + Blower	19	255.22	13.43263	0.047509

Table 3. Analysis of variance without replication by electrical efficiency

Source of Variation	SS	df	MS	F	P-value	F crit
Times of Experiment	14.07498	18	0.781943	27.05796	9.95E-21	1.798236
PV Configuration Cooling System	9.405063	3	3.135021	108.4826	7.58E-23	2.775762
Error	1.560537	54	0.028899			
Total	25.04058	75				

In contrast, the thermal efficiency trends summarized in Table 4 exhibit an opposite behavior to that of electrical efficiency. The PV-only configuration recorded the highest average thermal efficiency (81.55%) due to greater heat retention. In contrast, the PV + Heatsink and PV + Blower systems exhibited slightly lower values, likely due to enhanced heat dissipation. The lowest thermal efficiency was observed in the PV + Heatsink + Blower configuration (80.57%), indicating the most effective heat removal from the module. ANOVA in Table 5 confirms a strong influence of the cooling configuration on thermal efficiency ($F = 96.44 > F\text{-crit} = 2.77$, $p = 1.12 \times 10^{-21}$). The variance results further indicate that hybrid cooling yields the most stable thermal behavior, thereby ensuring consistent temperature regulation and maximizing electrical performance.

Table 4. Summary of experiment data by thermal efficiency

Summary	Count	Sum	Average	Variance
0	4	320.4	80.1	0
10	4	321.23	80.3075	0.010425
20	4	321.79	80.4475	0.046825
30	4	322.3	80.575	0.0867
40	4	323.06	80.765	0.098967
50	4	323.68	80.92	0.128333
60	4	324.07	81.0175	0.149092
70	4	324.44	81.11	0.179267

Table 4. *Cont.*

Summary	Count	Sum	Average	Variance
80	4	324.71	81.1775	0.200025
90	4	324.99	81.2475	0.219758
100	4	325.24	81.31	0.237467
110	4	325.45	81.3625	0.253692
120	4	325.61	81.4025	0.266758
130	4	325.75	81.4375	0.279558
140	4	325.87	81.4675	0.288158
150	4	325.99	81.4975	0.296892
160	4	326.11	81.5275	0.305758
170	4	326.2	81.55	0.318867
180	4	326.24	81.56	0.313133
PV Only	19	1549.53	81.55421	0.386281
PV+Heatsink	19	1540.56	81.08211	0.26894
PV+Blower	19	1542.17	81.16684	0.222334
PV+Heatsink+Blower	19	1530.87	80.57211	0.044762

Table 5. Analysis of variance without replication by thermal efficiency

Source of Variation	SS	df	MS	F	P-value	F crit
Times of Experiment	14.86537	18	0.825854	25.68402	3.38E-20	1.798236
PV Configuration Cooling System	9.302688	3	3.100896	96.43773	1.12E-21	2.775762
Error	1.736337	54	0.032154			
Total	25.90439	75				

The results of this study confirm that cooling configuration plays a decisive role in determining the electrical and thermal performance of photovoltaic modules under controlled irradiation. The hybrid PV + Heatsink + Blower system consistently delivered superior electrical efficiency, voltage stability, and power output by significantly reducing module temperature and maintaining favorable operating conditions. While the current production showed only minor sensitivity to temperature changes, voltage and power exhibited significant improvements, highlighting their dominant role in enhancing efficiency. ANOVA results further indicate that both cooling configuration and experimental duration significantly influence performance, emphasizing the dynamic nature of thermal accumulation during solar simulator testing. Despite these advantages, several limitations should be acknowledged and addressed in future work. The use of a halogen-based solar simulator with a spectrum that does not fully match the Air Mass 1.5 (AM1.5) standard may limit direct extrapolation to outdoor conditions, and the study was restricted to a single PV module type. Future investigations should explore multiple PV technologies and advanced cooling

strategies, such as phase-change materials, microchannel heatsinks, and liquid-based systems, to enable broader performance comparisons. Additionally, incorporating environmental variability and conducting long-term thermal cycling tests are crucial for evaluating the durability of photovoltaic applications.

4 Conclusions

This study investigated the thermal and electrical performance of a photovoltaic (PV) module under controlled solar simulator irradiation using four cooling configurations: PV Only, PV + Heatsink, PV + Blower, and PV + Heatsink + Blower. The hybrid configuration achieved the highest average electrical efficiency (13.43%), while the PV-only system showed the lowest efficiency (12.45%), with heatsink-only and blower-only systems providing moderate improvements. Voltage was identified as the most temperature-sensitive parameter, resulting in a higher power output of approximately 47.6 W in the hybrid system compared to about 43.0 W for the PV-only system. Thermally, the PV-only system exhibited the highest thermal efficiency (81.55%). In contrast, the hybrid system recorded the lowest value (80.57%), due to enhanced heat dissipation and a maximum temperature reduction of up to 35 °C. ANOVA results confirmed that cooling configuration significantly influences both electrical and thermal efficiencies, while experimental duration also affects performance due to progressive thermal accumulation. Although the hybrid PV + Heatsink + Blower system delivered the best electrical performance, it resulted in lower thermal efficiency, highlighting a clear trade-off between electrical enhancement and heat retention. Overall, the findings demonstrate that simple, low-energy cooling solutions can effectively enhance PV performance under simulated solar conditions. Future studies should consider AM1.5-compliant solar simulators, various PV technologies, advanced cooling methods, and long-term thermal cycling to further validate system reliability and applicability.

References

1. D. Colarossi, E. Tagliolini, P. Principi, and R. Fioretti, Design and Validation of an Adjustable Large-Scale Solar Simulator. *Appl. Sci.*, 11(4), 1964, 2021.
2. S. D. Prasetyo, Y. Trisnoaji, Z. Arifin and A. R. Prabowo, “Assessment of the performance differences in PV–PCM systems with numerical analysis of different phase change materials and structural designs,” *Sol. Energy Mater. Sol. Cells*, vol. 295, article no. 114019, 2026.
3. Y. Trisnoaji, S. D. Prasetyo, Z. Arifin and A. R. Prabowo, “Numerical investigation of photovoltaic–phase change material systems: Optimization of fin geometry for enhanced thermal management and solar panel performance,” *J. Energy Storage*, vol. 154, article no. 121126, 2026.
4. S. D. Prasetyo, Z. Arifin, M. S. Mauludin, Sukarman and M. Taufik, “Photovoltaic performance based on radiation intensity examination using experimental study and thermal simulation,” *Jurnal Teknik Mesin Mechanical Xplore / JTMMX* vol. 4, no. 2, pp. 86-97, 2024.
5. Wibawa Endra Juwana, Rendy Adhi Racmanto, Ubaidillah, Yuki Trisnoaji, Singgih Dwi Prasetyo, Zainal Arifin, “The role of fin–PCM integration in enhancing photovoltaic performance,” *Green Technol. Sustain.*, no. September, article no. 100306, 2025.
6. H. Attia, K. Hossin and M. Al Hazza, “Experimental investigation of photovoltaic systems for performance improvement using water cooling,” *Clean Energy*, vol. 7, no. 4, pp. 721-733, 2023.
7. T. Okamkpa, J. Okechukwu, D. Mbachu and C. Mgbemene, “Performance analysis of a photovoltaic system with thermoelectric generator and phase change material: An experimental approach,” *Adv. Sci. Technol.*, vol. 160, pp. 53-63, 2025.
8. S. A. Zubeer and O. Mohammed, “Performance analysis and electrical production of photovoltaic modules using active cooling system and reflectors,” *Ain Shams Eng. J.*, vol. 12, no. 2, pp. 2009-2016, 2021 .
9. M. Sharaf, M. S. Yousef and A. S. Huzayyin, “Review of cooling techniques used to enhance the efficiency of photovoltaic power systems,” *Environ. Sci. Pollut. Res.*, pp. 26131-26159, 2022.
10. M. Sheikholeslami and A. M. Alinia, “Simulation of solar panel system combined with NEPCM layer in existence of thermoelectric module,” *J. Therm. Anal. Calorim.*, vol. 150, no. 6, pp. 4325-4342, 2025.
11. X. Zhou, X. Cao, Z. Leng, X. Zhou and S. Liu, “Study on the temperature control performance of photovoltaic module by a novel phase change material/heat pipe coupled thermal management system,” *J. Energy Storage*, vol. 64, article no. 107200, 2023.
12. H. Metwally, N. A. Mahmoud, M. Ezzat and W. Aboelsoud, “Numerical investigation of photovoltaic hybrid

cooling system performance using thermoelectric generator and RT25 phase change material," *J. Energy Storage*, vol. 42, article no. 103031, 2021.
13. A. Kouravand, A. Kasaeian, F. Pourfayaz and M. A. Vaziri Rad, "Evaluation of a nanofluid-based concentrating photovoltaic thermal system integrated with finned PCM heatsink: An experimental study," *Renew. Energy*, vol. 201, pp. 1010-1025, 2022.
14. R. Salehi, A. Jahanbakhshi, J. B. Ooi, A. Rohani and M. R. Golzarian, "Study on the performance of solar cells cooled with heatsink and nanofluid added with aluminum nanoparticle," *Int. J. Thermofluids*, vol. 20, article no. 100445, 2023 .
15. A. Torbatinezhad, A. A. Ranjbar, M. Rahimi and M. Gorzin, "A new hybrid heatsink design for enhancement of PV cells performance," *Energy Rep.*, vol. 8, pp. 6764-6778, 2022.
16. A. Aljumaili, Y. Alaiwi and Z. Al-Khafaji, "Investigating back surface cooling system using phase change materials and heatsink on photovoltaic performance," *J. Eng. Sustain. Dev.*, vol. 28, no. 3, pp. 294–315, 2024.
17. A. R. Amelia, M. A. Jusoh and I. S. Idris, "Effect of thermoelectric cooling module and water flow heatsink on photovoltaic panel performance," *EPJ Web Conf.*, vol. 162, article no. 01077, 2017.
18. T. Abdelaty, H. N. Chaudhry, and J. K. Calautit, "Investigation of Cooling Techniques for Roof-Mounted Silicon Photovoltaic Panels in the Climate of the UAE: A Computational and Experimental Study," *Energies*, vol. 16, no. 18, article no. 6706, 2023.
19. V. S. Hudișteanu, N. C. Cherecheș, F. E. Țurcanu, I. Hudișteanu and C. Romila, "Impact of temperature on the efficiency of monocrystalline and polycrystalline photovoltaic panels: A comprehensive experimental analysis for sustainable energy solutions," *Sustain.*, vol. 16, no. 23, article no. 10566, 2024.
20. A. T. Mohammad and W. A. M. Al-Shohani, "Numerical and experimental investigation for analyzing the temperature influence on the performance of photovoltaic module," *AIMS Energy*, vol. 10, no. 5, pp. 1026-1045, 2022.
21. G. Raina, R. Vijay, "Assessing the suitability of I–V curve translation at varying irradiance and temperature range," *Sustain. Energy Technol. Assess.*, vol. 51, article no. 101925, 20222.
22. B. R. Paudyal and A. G. Imenes, "Investigation of temperature coefficients of PV modules through field measured data," *Sol. Energy*, vol. 224, pp. 425-439, 2021.
23. A. O. M. Maka and T. S. O'Donovan, "Effect of thermal load on performance parameters of solar concentrating photovoltaic systems," *Energy Built Environ.*, vol. 3, no. 2, pp. 201–209, 2022.
24. W. S. Ebhota and P. Y. Tabakov, "Influence of photovoltaic cell technologies and elevated temperature on photovoltaic system performance," *Ain Shams Eng. J.*, vol. 14, no. 7, article no. 101984, 2023.
25. L. O. A. Oyinkanola, O. A. Aremu, J. A. Fajemiroye and S. O. Makinde, "Dielectric response of castor oil processed in Nigeria as transformer insulating fluid," *Jurnal Internasional Penelitian dan Inovasi dalam Ilmu Terapan / IJRIAS* vol. VIII, pp. 60–66, 2023.
26. T. N. Olayiwola, S. H. Hyun and S. J. Choi, "Photovoltaic modeling: A comprehensive analysis of the I–V characteristic curve," *Sustain.*, vol. 16, no. 1, pp. 1–27, 2024.
27. D. Zhang, D. Li, Y. Hu, A. Mei and H. Han, "Degradation pathways in perovskite solar cells and how to meet international standards," *Comm. Mat.*, vol. 3, no. 1, article no. 58, 2022.
28. A. J. Sexton, H. Qandil, M. Abdallah and W. Zhao, "Investigation of non-imaging Fresnel lens prototyping with different manufacturing methods for solar energy application," *J. Mech. Energy Eng.*, vol. 5, no. 2, pp. 113-122, 2021.
29. A. M. Rheima, A. G. Sager, M. A. Mohammed and A. J. Mahdi, "Fabrication of dye-sensitized solar cell using CuO nanoparticles as photoanode," *Baghdad Sci. J.*, vol. 22, no. 7, pp. 2133–2143, 2025 .
30. F. Saeed and A. Zohaib, "Quantification of losses in a photovoltaic system: A review," *Eng. Proc.*, vol. 11, no. 1, pp. 4–9, 2021.
31. M. Dörenkämper, M. M. de Jong, J. Kroon, V. S. Nysted, J. Selj and T. Kjeldstad, "Modeled and measured operating temperatures of floating PV modules: A comparison," *Energies*, vol. 16, no. 20, article no. 7153, 2023.
32. S. Z. Islam, M. L. Othman, M. Saufi, R. Omar, A. Toudeshki and S. Z. Islam, "Photovoltaic modules evaluation and dry-season energy yield prediction model for NEM in Malaysia," *PLoS One*, vol. 15, no. 11, article no. 0241927, 2020.